Liu *et al. Stem Cell Research & Therapy* (2025) 16:240
https://doi.org/10.1186/s13287-025-04368-5

Stem Cell Research & Therapy

RESEARCH Open Access

Human dental pulp stem cells attenuate airway inflammation in mice with $PM_{2.5}$-induced asthma exacerbation by inhibiting the pyroptosis pathway

Jianling Liu[1,2†], Yuehua Chen[1†], Zhongpeng Li[3], Zhangwen Li[1,2], Fengjuan Lyu[4,5], Fang Wang[1,2], Aili Wang[1], Zhangquan Liu[1], Xiaoyang Liao[1] and Jian Wu[1,2*]

Abstract

Background Fine particulate matter ($PM_{2.5}$) exposure significantly exacerbates respiratory morbidity, particularly in asthmatic individuals, highlighting an urgent need for effective therapeutic interventions. In this study, we evaluated the therapeutic potential and underlying mechanisms of human dental pulp stem cells (hDPSCs), a promising mesenchymal stem cell population, in mitigating airway inflammation in mice with $PM_{2.5}$-induced asthma exacerbation.

Methods In a $PM_{2.5}$-exacerbated ovalbumin (OVA)-asthma murine model, hDPSCs were intravenously administered with MCC950 (NLRP3 inhibitor) as positive control, systematically evaluating their therapeutic effects on airway inflammation and pyroptosis through pulmonary function tests, histopathological examination, cytological and molecular analyses.

Results The administration of hDPSCs ameliorated airway inflammation. Moreover, hDPSCs further alleviated Th2 inflammation and decreased serum IgE concentrations, along with a decrease in eosinophils in BALF. At the same time, interleukin-1β (IL-1β) and IL-18 levels in BALF and caspase-1 activity in lung tissues were reduced. In addition, immunohistochemistry showed that the expression levels of NLRP3, caspase-1, GSDMD, cleaved capsase-1 and IL-1β were reduced. The western blot results also showed that the expression level of NLRP3/caspase-1/GSDMD/cleaved capsase-1 in the classical pathway of pyroptosis decreased after hDPSCs intervention.

Conclusions These findings provided the first evidence that hDPSCs transplantation attenuated allergic airway inflammation and mucus secretion in mice with $PM_{2.5}$-induced asthma exacerbation. Thus, hDPSCs exert these protective effects through suppression of the NLRP3/caspase-1/GSDMD-mediated pyroptosis pathway, suggesting their potential as a novel cell-based therapy for $PM_{2.5}$ inhalation-mediated asthma.

†Jianling Liu and Yuehua Chen contributed equally to this work as co-first authors.

*Correspondence:
Jian Wu
sywujian@scut.edu.cn

Full list of author information is available at the end of the article

Keywords Human dental pulp stem cells, Airway inflammation, $PM_{2.5}$-induced asthma exacerbation, Pyroptosis, Cell therapy

Introduction

Asthma is a chronic inflammatory disease that affects hundreds of millions of people worldwide [1]. It is distinguished by an increase in type 2 immune cells that infiltrate the airways, such as mast cells, basophils, eosinophils, and T helper 2 (Th2) cells, which render excessive mucus production and airway hyperresponsiveness (AHR), ultimately leading to airflow obstruction [2, 3]. Environmental factors, such as air pollution, are one of the main causes of asthma attack and exacerbation [4]. $PM_{2.5}$ is particulate matter, the main component of air pollution, with an aerodynamic diameter of less than 2.5 [5, 6]. Due to its ability to spread further into the terminal bronchioles and alveoli, $PM_{2.5}$ is considered particularly detrimental in triggering asthma attacks [7]. While the precise mechanism by which $PM_{2.5}$ causes asthma exacerbations is still unknown, emerging evidence implicates $PM_{2.5}$-induced activation of the nod-like receptor pyrin domain containing 3 (NLRP3) inflammasome and subsequent pyroptosis in asthma exacerbation pathogenesis [8, 9].

Pyroptosis is a novel type of inflammatory and programmed cell death, characterized by cellular enlargement, membrane rupture, and the release of immune-stimulating substances from the cell [10]. The recognition receptor known as the NLRP3 inflammasome is responsible for the creation of inflammatory vesicles, which are made up of many complexes including NLRP3, caspase-1 and proteins containing the C-terminal cysteoaspartate-recruiting structural domain (ASC). Activation of NLRP3 inflammasome activates caspase-1 and other cysteoaspartic enzymes, which in turn cleave the GSDMD, releasing its N-terminus, leading to rupture and perforation of the cell membrane and the release of cytokines such as IL-1β and IL-18, leading to pyroptosis [11]. NLRP3 inflammasome-mediated pyroptosis is closely associated with respiratory diseases [12]. Notably, the selective NLRP3 inhibitor MCC950 has been shown to attenuate lung injury and ischemia/reperfusion-induced inflammasome activation [13]. Emerging studies specifically demonstrated that $PM_{2.5}$ exposure triggers NLRP3-inflammasome-mediated pyroptosis in pulmonary tissues [14]. For example, Juan Li et al. discovered that the $PM_{2.5}$ exposure activated NLRP3 inflammasome in airway epithelial cells, which was linked to the pathophysiology of lung inflammation [15]. Another study also reported $PM_{2.5}$ led to lung damage by activating the NLRP3 inflammasome and promoting pyroptosis [16]. Therefore, targeting NLRP3 inflammasome-mediated pyroptosis might be a potential treatment for asthma.

Mesenchymal stem cells are pluripotent stem cells derived from multiple sources [17, 18], such as bone marrow [19], adipose tissue [20], umbilical cord, and placenta [21], with distinct differences in differentiation potency and cytokine profiles [22]. It has been demonstrated to have anti-inflammatory [23], anti-fibrotic [24], and immunomodulatory properties [25]. Dental pulp stem cells (DPSCs) have similar immunophenotypic and multidirectional differentiation characteristics to MSCs, but DPSCs exhibited higher proliferation rate [26, 27]. DPSCs offer distinct advantages for therapeutic applications, including accessibility, absence of ethical constraints, potent bioactivity, low immunogenicity, and robust differentiation potential [28]. These cells exhibit significant anti-inflammatory properties in various pathological conditions such as inflammatory bowel disease and peripheral neuropathy [29]. Notably, in paraquat-induced acute respiratory distress syndrome, DPSCs demonstrate enhanced anti-inflammatory efficacy compared to umbilical cord-derived MSCs [30]. Supporting these findings, Gao et al. reported that intratracheally administered DPSCs ameliorated pulmonary function, attenuated emphysematous changes, and reduced inflammation in a murine chronic obstructive pulmonary disease (COPD) model through Nrf2 pathway activation and oxidative stress suppression [31].

Currently, it is unclear whether human DPSCs (hDPSCs) may have potential in preventing $PM_{2.5}$-exacerbated asthma lung injury. This study aimed to investigate whether hDPSCs exert a protective effect against $PM_{2.5}$-induced inflammation by suppressing pyroptosis.

Materials and methods

Cell culture and characterization of hDPSCs

Human dental pulp stem cells (OriCell®, Guangzhou, China) were provided by Cyagen Biosciences (Guangzhou) Inc, with donor informed consent obtained. The hDPSCs were cultured in stem cell-specific medium (OriCell®, Guangzhou, China) supplemented with 10% fetal bovine serum (FBS). Flow cytometry identification of DPSCs was performed using the Mesenchymal Stem Cell Surface Marker Assay Kit (OriCell®, Guangzhou, China). To assess multilineage differentiation potential, hDPSCs were cultured in differentiation media according to the instructions of the Osteogenesis, Adipogenic and Chondrogenic Kit (OriCell®, Guangzhou, China), followed by staining with alizarin red, oil red O, and alcian blue to confirm successful induction of osteogenesis, adipogenesis, and chondrogenesis.

Preparation of $PM_{2.5}$

$PM_{2.5}$ samples were collected from January 2 to March 16, 2022, using the American TISCH high-flow atmospheric sampler (Thermo Fischer Scientific, Waltham, USA) at the Guangzhou Institute of Geochemistry, Chinese Academy of Sciences (Guangzhou, China). Quartz filter membranes were sectioned into 3 × 3 cm pieces, ultrasonically extracted in 500 mL deionized water (three 30-minute cycles), and filtered through eight-layer gauze. The filtrate was subsequently centrifuged at 4 °C, 9000 rpm for 1 h, and the resulting precipitate was refrigerated for 48 h before vacuum freeze-drying for 36 h to remove residual moisture. The $PM_{2.5}$ composition was validated against standard reference materials from the National Institute of Standards and Technology (NIST), with certified mass fractions of organic and inorganic components determined by high-performance liquid chromatography [32].

Animals and ethics statements

Specific-pathogen-free female BALB/c mice (6–8 weeks old, weight = 18–22 g) were purchased from Guangdong Scarstar Biotechnology Co., Ltd (License No.: SCXK2020-0052). The mice were fed in the Animal Experiment Center of South China University of Technology with ad libitum access to autoclaved water and standard rodent diet. All animal protocols, including the use of human cells to intervene mice, were approved by the Animal Welfare and Use Committee of the South China University of Technology (Approval ID: 2023051).

Experimental design of animal studies

Fifty female BALB/c mice were randomly allocated into five groups (10 mice per group): control group, OVA group, OVA + $PM_{2.5}$ group, OVA + $PM_{2.5}$ + MCC950 (the NLRP3 inhibitor) group, OVA + $PM_{2.5}$ + hDPSCs group. Ovalbumin (OVA) is a common allergen. And the asthma model was sensitized and challenged using OVA according to the previous study protocol [33, 34]. As illustrated in Fig. 1A, mice were sensitized via intraperitoneal injection of a mixture containing 50 μg ovalbumin (OVA; Sigma-Aldrich, St. Louis, USA) and 5 mg aluminum hydroxide (Sigma-Aldrich) on days 1, 7, and 14. Subsequently, from days 21 to 27, animals were subjected to daily 30-minute challenges with 2% OVA aerosol using a compressor nebulizer (402AI, JS, China) every day. Thirty minutes prior to each OVA nebulization, 20 μL of 5 mg/mL $PM_{2.5}$ suspension in 0.9% saline was administered intranasally. MCC950 is an NLRP3-specific inhibitor and was used as a positive control group in this study [35]. On days 21 and 24, OVA + $PM_{2.5}$ + MCC950 group and OVA + $PM_{2.5}$ + hDPSCs group mice received intravenous injections of either hDPSCs (1 × 10^6 cells in 200 μL PBS) or MCC950 (50 mg/kg, GLPBIO, USA). The hDPSC dosage was determined based on established protocols [30, 36], while the MCC950 dose followed manufacturer specifications. On the 28th day, mice were tested for pulmonary function. Then mice were euthanized by intravenous injection of pentobarbital sodium (120 mg/kg).

Pulmonary function test

Pulmonary function was assessed within 24 h after the final $PM_{2.5}$ exposure using a FinePointe whole-body plethysmography (WBP) system (DSI Instrument Co., Ltd, ST. PAUL, USA). Following device calibration, mice were acclimated in the whole-body chamber for 3 min prior to testing. Airway responsiveness was evaluated through sequential nebulization of acetylcholine at increasing concentrations (0, 6.25, 12.5, 25, and 50 mg/mL), with each concentration administered for 30 s followed by a 3-min recording period. Airway hyperresponsiveness was quantified using the enhanced pause (Penh) index.

Measurement of inflammatory cytokines in Bronchoalveolar lavage fluid

Mice were anesthetized with 1% pentobarbital sodium and intubated using a 0.8-gauge flexible catheter connected to a 1 mL syringe for bronchoalveolar lavage fluid (BALF) collection. Then, 0.8 mL of ice-cold sterile PBS was instilled into the lungs and slowly withdrawn to obtain approximately 0.5 mL of BALF following gentle thoracic massage. This lavage procedure was repeated twice. The pooled BALF was centrifuged at 3000 rpm for 10 min at 4 °C, and the resulting cell pellet was resuspended in PBS for counting using a hemocytometer under light microscopy. The supernatant was aliquoted and stored at -80 °C for subsequent analysis. Differential cell counts were performed using modified Giemsa stain (Servicebio, Wuhan, China). Total protein concentration was quantified using a BCA assay kit, while cytokine levels were determined by ELISA (Cusabio, Houston, TX, USA) and multiplex immunoassay (LabEx).

Measurement of serum immunoglobulin E (IgE)

The peripheral blood of mice was collected, left at 4 °C for 12 h, and centrifuged at 3000 rpm at 4 °C for 10 min to obtain serum. Serum IgE concentrations were determined using an enzyme-linked immunosorbent assay kit (Solarbio, Beijing, China).

Histological evaluation and immunohistochemistry analysis

The left lungs were fixed via tracheal perfusion with 4% paraformaldehyde (PFA) and post-fixed for 48 h before paraffin embedding. Serial 5 μm sections were prepared and stained with periodic acid-Schiff (PAS) and hematoxylin-eosin (H&E). Histopathological scoring criteria

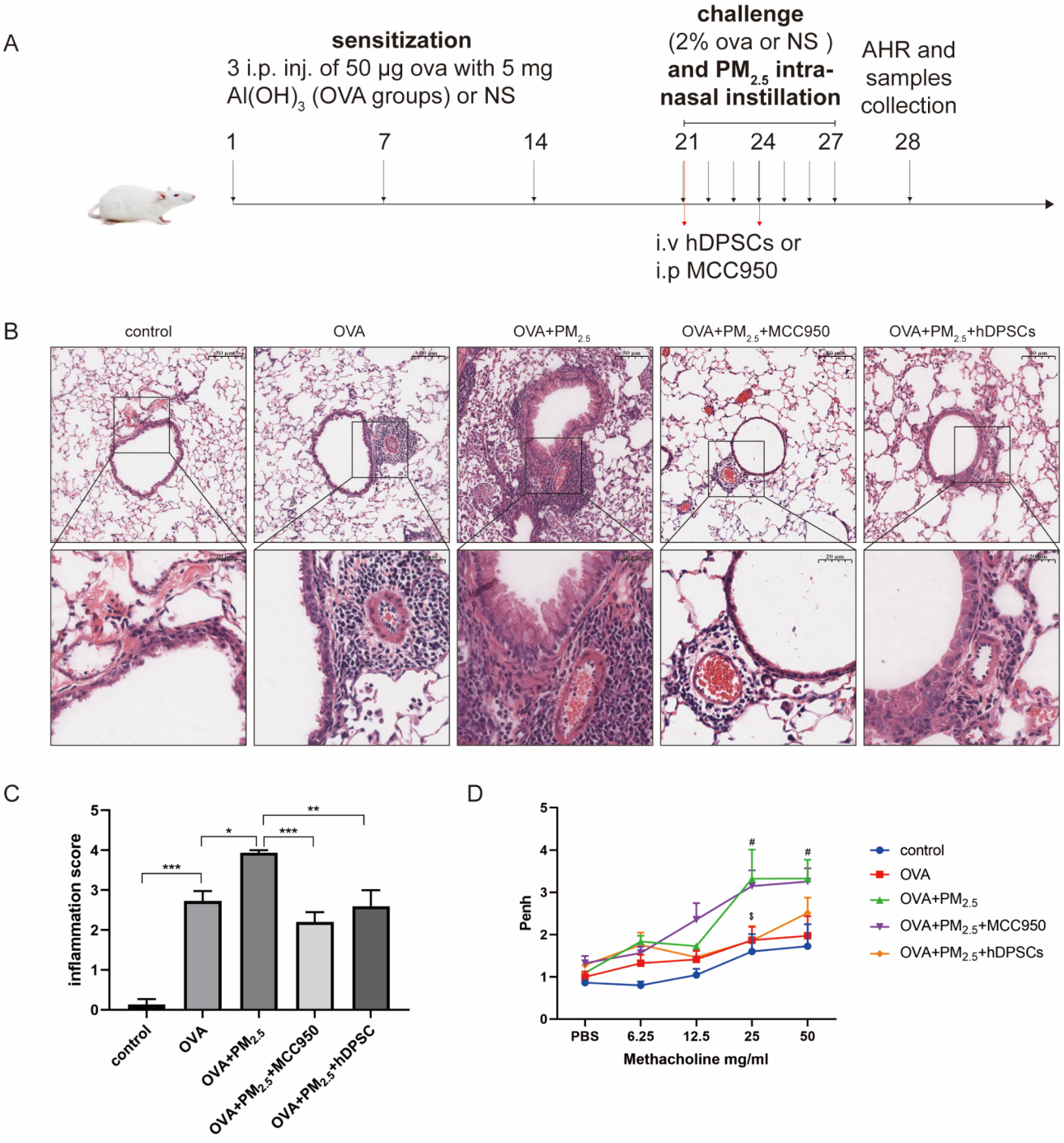

Fig. 1 Lung inflammation and airway responsiveness. (**A**) Experimental design. (**B**) Representative images of H&E stained lung sections from each group (scale bar: up: 50 μm; down:20 μm). (**C**) The inflammatory infiltration was quantified by HE scores ($n = 5$/group). (**D**) Airway responsiveness of mice ($n = 4$/group). *: vs. OVA group; #: vs. OVA+$PM_{2.5}$ group

was as follows: 0 points: no significant inflammation; 1 point: a small number of inflammatory cells; 2 points: a thin layer of inflammatory cells; 3 points: inflammatory cell infiltration in 2–4 layers; Score 4: Inflammatory cell infiltration above 4 layers [37, 38].

Lung tissue sections were subjected to immunohistochemical (IHC) staining to evaluate the expression of NLRP3, caspase-1, GSDMD, cleaved caspase-1, and IL-1β proteins. Following standard paraffin embedding and dehydration, antigen retrieval was performed using citrate buffer (pH 6.0). Subsequently, the slices were blocked with 10% goat serum for 30 min prior to incubation with caspase-1 (1:100, Origene), NLRP3 (1:200, Servicebio), GSDMD (1:100, Affinity), cleaved caspase-1

(1:100, Servicebio), and IL-1β (1:100, Servicebio) antibodies at 4 °C overnight. After washes in PBS immersion, the slides were incubated with goat horseradish conjugated goat anti-rabbit IgG secondary antibody (1:100, Servicebio) for 2 h at room temperature. Counterstain was achieved by incubation with 3,3′-diaminobenzidine (DAB) for 15 min. Protein expression was quantified in three randomly selected fields per slide using ImageJ software, with results expressed as mean absorbance and average absorbance (absorbance/positive area).

Caspase-1 activity assessment

According to the Caspase-1 Activity Assay Kit (Beyotime, Shanghai, China), the mice's pulmonary tissue was split on the ice and decentralized. After incubated with caspase-1 substrate for 2 h at 37 °C, the level of yellow-methane products of nitrogen-benzamine (pNA) was measured at 450 nm.

Western blot

Proteins from lung tissues were extracted with RIPA lysis buffer (Beyotime, Shanghai, China). and quantified with a BCA Protein Assay Kit. The lysates (30 μg/lane) were electrophoresed on a 4–12% SDS-PAGE gel and transferred to polyvinylidene difluoride (PVDF) membranes ((Millipore, Billerica, MA, USA). After blocking with 5% milk/ Tris Buffered Saline/0.01% Tween (TBST) for 2 h at room temperature, membranes were further incubated with primary antibodies against NLRP3 (1:1000; CST), caspase-1 (1:1000; CST), GSDMD (1:1000; CST) or GAPDH (1:2000; Absin) overnight at 4 ℃. Following three TBST washes, membranes were incubated with HRP conjugated goat anti-rabbit IgG antibodies (1:5000; CST) for 2 h at room temperature. Finally, bands were detected using an ECL kit (Beyotime, Shanghai, China) and taken using a ChemiScope series (Clinx, Shanghai, China). The expression was quantified with Image J software and normalized to GAPDH.

Statistical analysis

All data were expressed as the mean ± SEM. Statistical analyses were performed using GraphPad Prism 8.0 for Windows (La Jolla, CA, USA). Statistical differences between three or more variables were calculated by analysis of variance (ANOVA) followed by Tukey's post hoc test. Statistical significance was determined using the following criteria: $^{*}P < 0.05$; $^{**}P < 0.01$; $^{***}P < 0.001$.

The work has been reported in line with the ARRIVE guidelines 2.0.

Results

Characterization of hDPSCs

HDPSCs adhered to the dish and displayed fibroblast-like morphology (Fig. 2A). Flow cytometry analysis revealed high expression of CD44 (99.88%) and CD146 (92.90%), with minimal expression of hematopoietic markers CD34 (0.30%) and CD45 (Fig. 2B). These results confirmed the predominantly non-hematopoietic MSC phenotype of the isolated cells. In differentiation assay, calcium nodules were stained in alizarin in osteogenic induction (Fig. 2C), red droplets were observed and stained with Oil Red O in adipogenic induction (Fig. 2D), and proteoglycan accumulation was observed with alcian blue staining in chondrogenic induction (Fig. 2E), which confirmed that hDPSCs can differentiate into osteocytes, adipocytes and chondrocytes.

Lung inflammation and airway responsiveness

The lung tissue of the control group exhibited an intact, well-organized bronchial structure, with few inflammatory cell infiltration observed around the bronchioles. The OVA group showed inflammatory exudation in the alveolar lumen, and plenty of inflammatory cells aggregated around the bronchioles and blood vessels. In the OVA + $PM_{2.5}$ group, there was thickening of the bronchiolar epithelial basement membrane and a significant inflammatory cell aggregation surrounding the bronchioles and blood vessels. The intervention of MCC950 or hDPSCs, reduced bronchial and perivascular inflammatory cell infiltration caused by OVA + $PM_{2.5}$ (Fig. 1B). The scores for lung injury were consistent with the above findings (Fig. 1C). Overall, $PM_{2.5}$-exposed mice had more inflammatory cells infiltration around blood vessels and bronchioles than the OVA group mice ($P < 0.05$). In addition, compared with the $PM_{2.5}$ group, the hDPSCs group had significantly lower tissue scores ($P < 0.01$). These results suggest that hDPSCs reduced pathological lung tissue damage in $PM_{2.5}$-induced asthma mouse episodes.

The results of pulmonary function test indicated that as the concentration of methacholine rose, the AHR of mouse steadily increased (Fig. 1D). Furthermore, the Penh values curve of hDPSCs climbed slowly, whereas the Penh values curve exhibited a larger and more significant increase following the $PM_{2.5}$ intervention. When the concentration of methacholine on 25 mg/mL and 50 mg/mL, the Penh values in the OVA + $PM_{2.5}$ group were substantially greater than those in the OVA group ($P = 0.0119$, $P = 0.0224$), showing that $PM_{2.5}$ intervention raised the AHR of asthma mouse. HDPSCs intervention reduced Penh values of the OVA + $PM_{2.5}$ group, and the difference became statistically significant when methacholine concentrations reached 25 mg/mL ($P = 0.0111$). However, there was no significant difference between the MCC950 group and the OVA + $PM_{2.5}$ group, indicating that MCC950 alone did not reduce AHR.

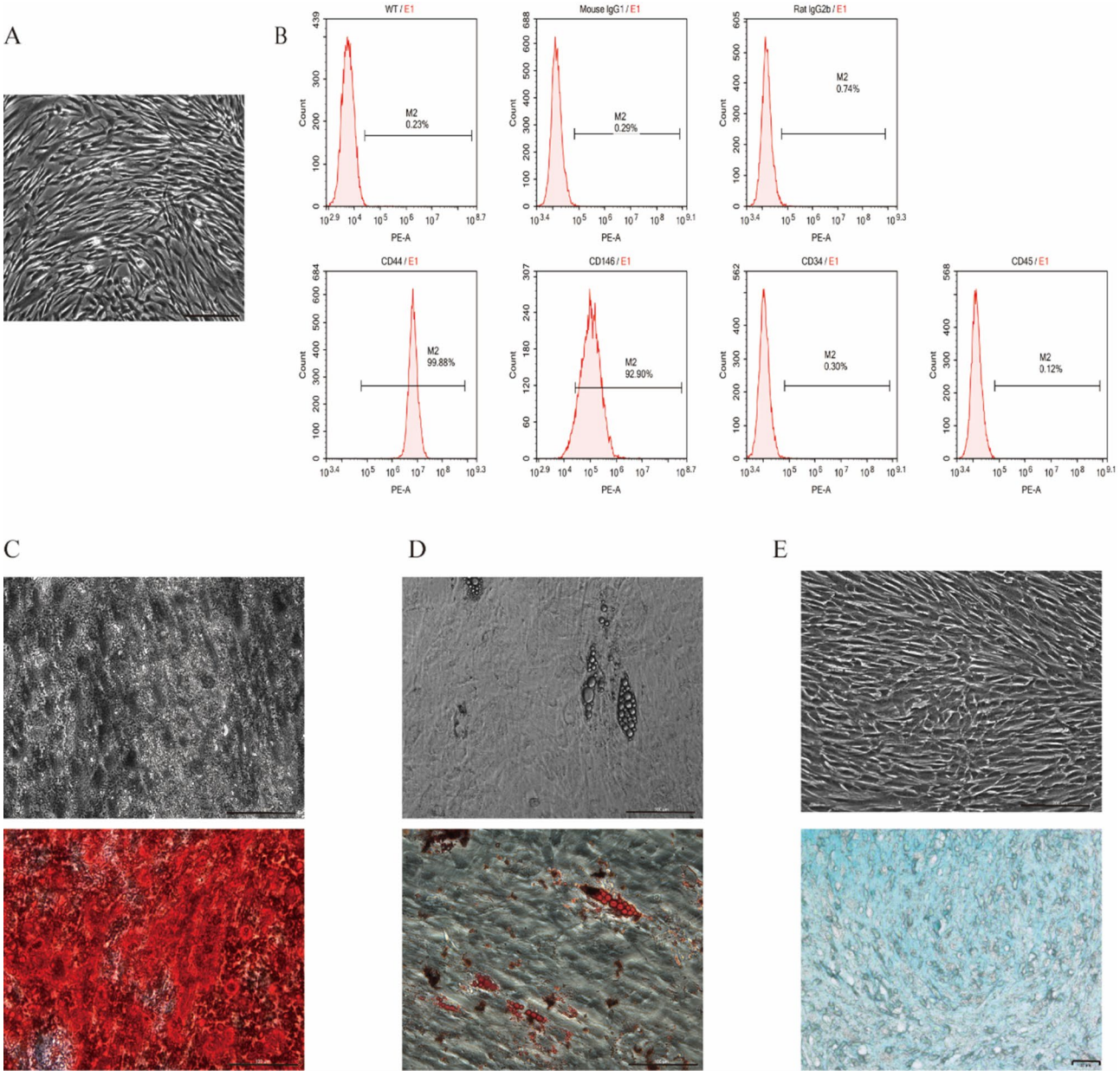

Fig. 2 Characterisation of hDPSCs. (**A**) Morphology of hDPSCs under 100x light microscope. (**B**) Surface expression of CD44, CD146, CD34, and CD45. (**C**) Alizarin red staining of hDPSCs on day 26. Up: before staining, blow: after staining. (**D**) Oil Red O staining of hDPSCs on day 21. Up: before staining, blow: after staining. (**E**) Alcian staining of hDPSCs on day 69. Up: before induction, blow: after induction

Goblet cell hyperplasia

Goblet cell proliferation and airway mucus secretion are characteristic hallmarks of allergic asthma, which could be assessed by PAS staining [39] As expected, intense PAS staining, a hallmark of goblet cell proliferation, was observed in mice with $PM_{2.5}$-induced exacerbation of allergic asthma (Fig. 3A). In addition, MCC950 infusion attenuated $PM_{2.5}$-induced goblet cell proliferation and airway mucus secretion ($P<0.001$). HDPSCs had similar effects to MCC950 in that they alleviate goblet cell hyperplasia and mucus secretion ($P<0.001$, Fig. 3B).

Disruption of the airway epithelial barrier facilitates extravasation of protein-rich fluid from the vasculature into pulmonary tissues [40]. Quantitative analysis of BALF revealed that $PM_{2.5}$ exposure significantly increased protein leakage compared with the OVA group ($P<0.05$), while both hDPSC transplantation and MCC950 administration effectively attenuated this effect ($P<0.001$, Fig. 3C). The results suggest that hDPSCs inhibit goblet cell proliferation and mucus secretion in the lungs as well as protect the intrapulmonary epithelial barrier.

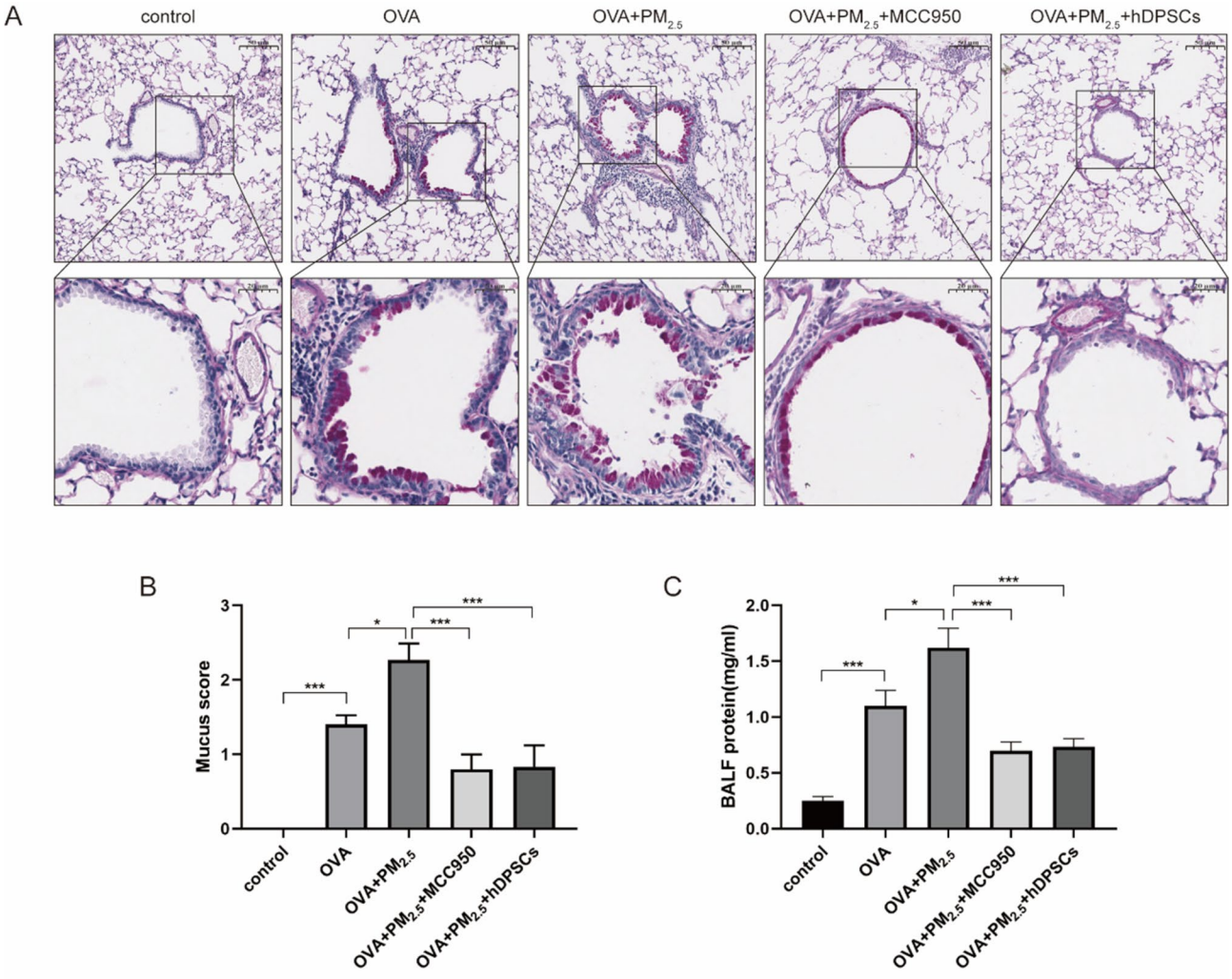

Fig. 3 Mucus secretion. (**A**) Representative images of PAS staining (scale bar: up: 50 μm; down:20 μm). (**B**) Quantitative analysis of mucus secretion. (**C**) Total protein concentration in BALF. ($n = 3$–5/group)

Serum IgE and pulmonary Th2 cytokines

Given that allergic asthma is characterized by Th2-biased immune responses [41, 42], we evaluated the impact of hDPSCs on Th2 cytokine production [41, 42]. Concurrently, serum IgE levels and inflammatory cell counts in BALF were quantified to assess inflammatory responses. Compared with the OVA group, increased levels of TNF-α and type 2 cytokines (IL-5 and IL-13) in the OVA + $PM_{2.5}$ group were observed ($P < 0.01$, $P < 0.05$). However, hDPSC intervention dramatically lowered their levels in BALF (both $P < 0.05$). Similarly, $PM_{2.5}$ exposure increased peripheral blood IgE levels compared to the OVA group ($P = 0.0960$), however, this increase could be reversed by hDPSCs ($P < 0.001$).

The number of total inflammatory cells and eosinophils in BALF was significantly increased in the OVA + $PM_{2.5}$ group compared to the OVA group ($P < 0.05$, Fig. 4E-F). Intravenous injections of hDPSCs (1×10^6 cells) in $PM_{2.5}$-treated mice reduced the total number of inflammatory cells in BALF ($P < 0.05$), particularly the eosinophils when compared to the PM2.5-treated mice ($P < 0.05$, Fig. 4F).

MCC950 also reduced IL-5 levels ($P < 0.01$), however, it did not significantly alter IL-4, IL-13, TNF-α, or IgE levels. At the same time, MCC950 did not change the number of BALF total cells and eosinophils in $PM_{2.5}$-induced asthma exacerbation. These results demonstrate that hDPSCs exhibit superior efficacy to MCC950 in attenuating pulmonary inflammation.

The expression of NLRP3 in the lungs

Pyroptosis plays an important role in inflammation [43]. To elucidate the mechanisms underlying hDPSCs-mediated attenuation of airway inflammation in $PM_{2.5}$-induced asthma exacerbation, we investigated the potential involvement of pyroptosis. NLRP3 expression

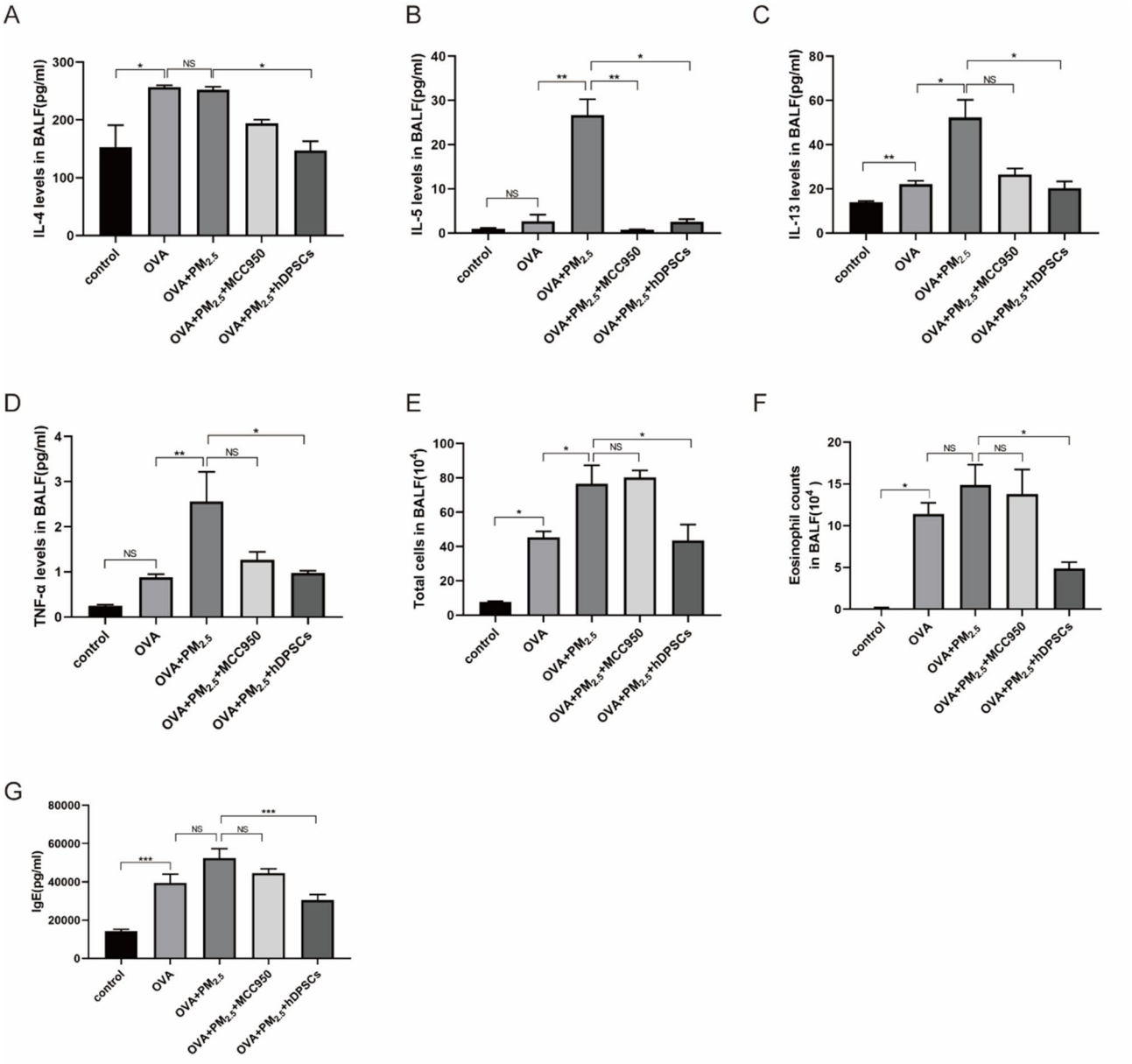

Fig. 4 Th2 immune response. (**A-D**) The levels of Th2-related cytokines and TNF-α were measured using ELISA. (**E-F**) Statistical analysis of the total cells and eosinophils in BALF. (**G**) Serum IgE levels were measured using ELISA. ($n = 3$–5/group)

was evaluated by IHC, while IL-1β and IL-18 levels were quantified using ELISA. Our results showed that compared with the OVA + $PM_{2.5}$ group, the proportion of NLRP3-positive cells was significantly reduced with the treatment of hDPSCs ($P < 0.05$, Fig. 5A). In addition, $PM_{2.5}$ exposure markedly elevated IL-1β and IL-18 concentrations compared to OVA treatment alone ($P < 0.01$, $P < 0.001$). Consistent with previous studies, MCC950 administration significantly downregulated NLRP3, IL-1β, and IL-18 expression versus the OVA + $PM_{2.5}$ group ($P < 0.05$, $P < 0.01$, $P < 0.001$). With the infusion of hDPSCs, the expression of IL-1β and IL-18 were decreased compared to the OVA + $PM_{2.5}$ group ($P < 0.05$, $P < 0.001$, Fig. 5C-D). These findings collectively demonstrate that hDPSCs ameliorate pulmonary inflammation by inhibiting NLRP3 inflammatory activation.

The NLRP3/caspase-1/GSDMD pathway reactivity

To investigate pyroptosis pathway activation in pulmonary tissues, we performed IHC and western blot analyses. IHC revealed that $PM_{2.5}$ exposure following OVA sensitization significantly upregulated pyroptosis-related proteins. Both MCC950 treatment and hDPSC administration effectively reduced expression levels of NLRP3 inflammasome downstream effectors, including caspase-1, GSDMD, cleaved caspase-1, and IL-1β (all the

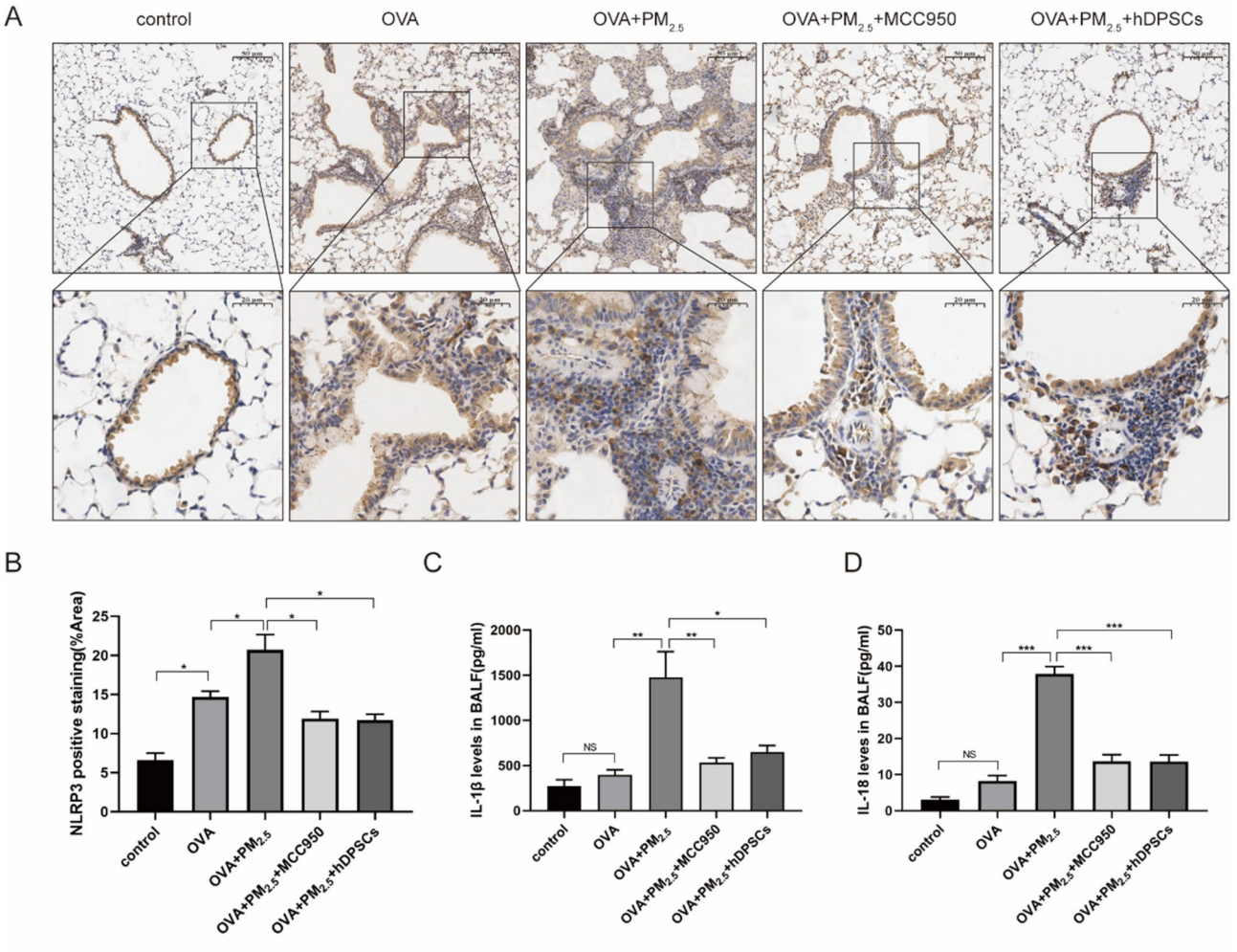

Fig. 5 The expression of NLRP3. (**A**) Representative images of NLRP3 immunohistochemical staining (scale bar: up: 50 μm; down:20 μm). (**B**) Quantification of NLRP3 staining in the lungs. (**C-D**) The expression of IL-1β and IL-18 in the lungs was analyzed using an ELISA assay. ($n = 3$/group)

$P < 0.05$, Fig. 6A), as quantified by immunohistochemical scoring (Fig. 6B-E).

Western blot analysis demonstrated significant upregulation of NLRP3, caspase-1, GSDMD, and cleaved caspase-1 protein expression in the OVA + $PM_{2.5}$ group compared to OVA group (all the $P < 0.05$, Fig. 7A). Notably, hDPSC infusion markedly downregulated these proteins relative to the OVA + $PM_{2.5}$ group (all the $P < 0.05$, Fig. 7C-F). Although $PM_{2.5}$ exposure increased caspase-1 activity, this change did not reach statistical significance. In contrast, both MCC950 and hDPSC interventions significantly suppressed caspase-1 activity (Fig. 7B).

These findings showed that hDPSCs had a mechanism of effect similar to the NLRP3 inhibitor MCC950, implying that hDPSCs decrease airway inflammation by inhibiting pyroptosis.

Discussion

In this study, we reported that $PM_{2.5}$ promoted experimental asthma development and was associated with pyroptosis, while hDPSCs prevented pyroptosis, attenuated airway inflammation and injury in $PM_{2.5}$-induced asthma exacerbation. The expression of NLRP3, caspase-1, GSDMD and cleaved caspase-1 were elevated after $PM_{2.5}$ administration, while hDPSCs inhibited the expression of proteins related to pyroptosis. MCC950 is an NLRP3-specific inhibitor and was used as a positive control group in this study [35]. The therapeutic impact of hDPSC infusion on asthma was comparable to that of MCC950. These data demonstrate that hDPSCs significantly attenuated $PM_{2.5}$-induced airway inflammation and reduced NLRP3 inflammasome activation suggesting their potential as a therapeutic candidate for $PM_{2.5}$-aggravated asthma.

Asthma is characterized by an infiltration of inflammatory cells, including eosinophils, and the release of inflammatory chemicals. OVA with aluminum hydroxide

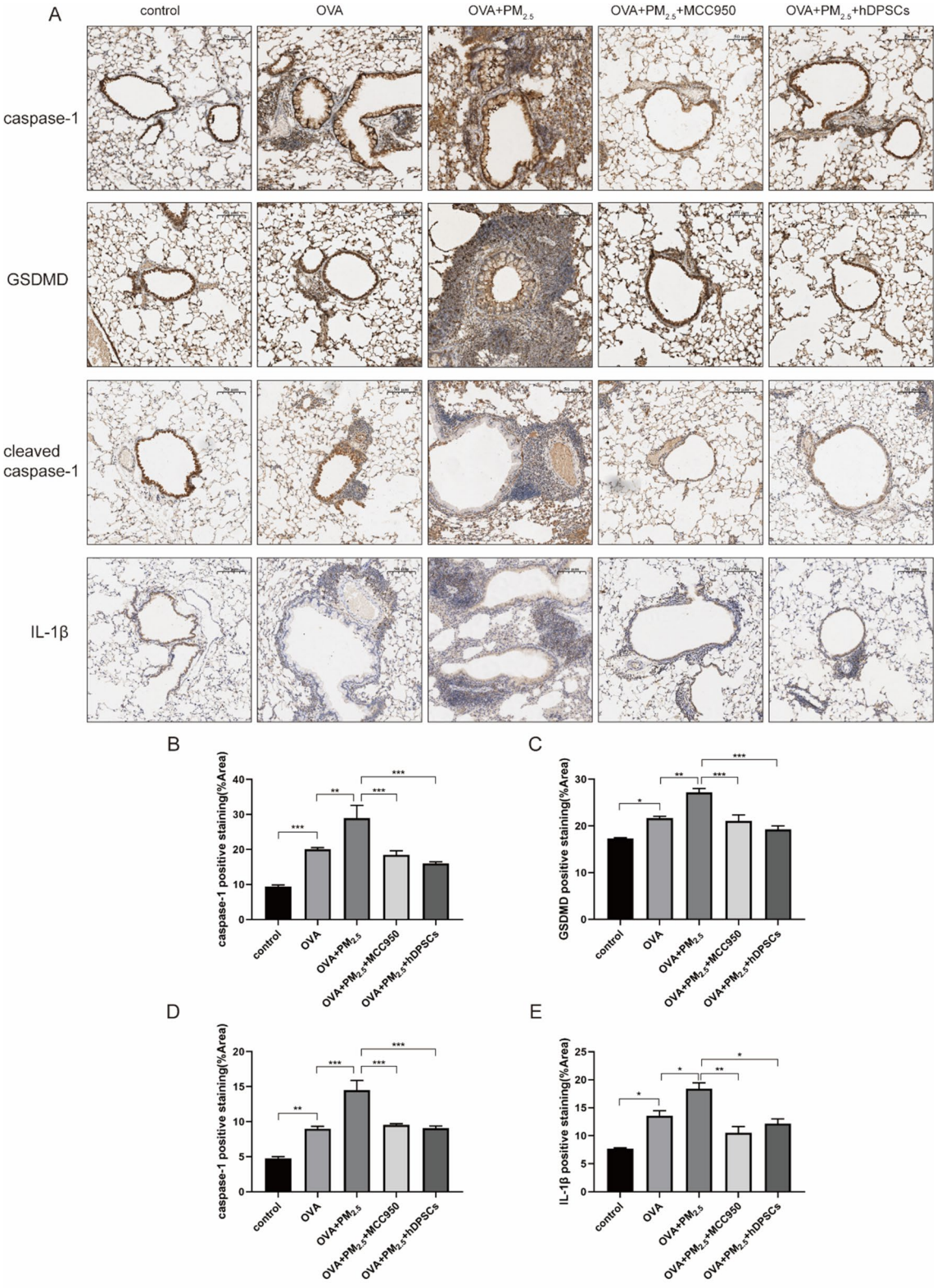

Fig. 6 Caspase-1, GSDMD, cleaved caspase-1 and IL-1β expression levels in the lungs. (**A**) Representative images of caspase-1/GSDMD/cleaved caspase-1/IL-1β immunohistochemical staining (scale bar: 50 μm). (**B-E**) Quantification of caspase-1/GSDMD/cleaved caspase-1/IL-1β staining in the lungs. ($n = 3–5$/group)

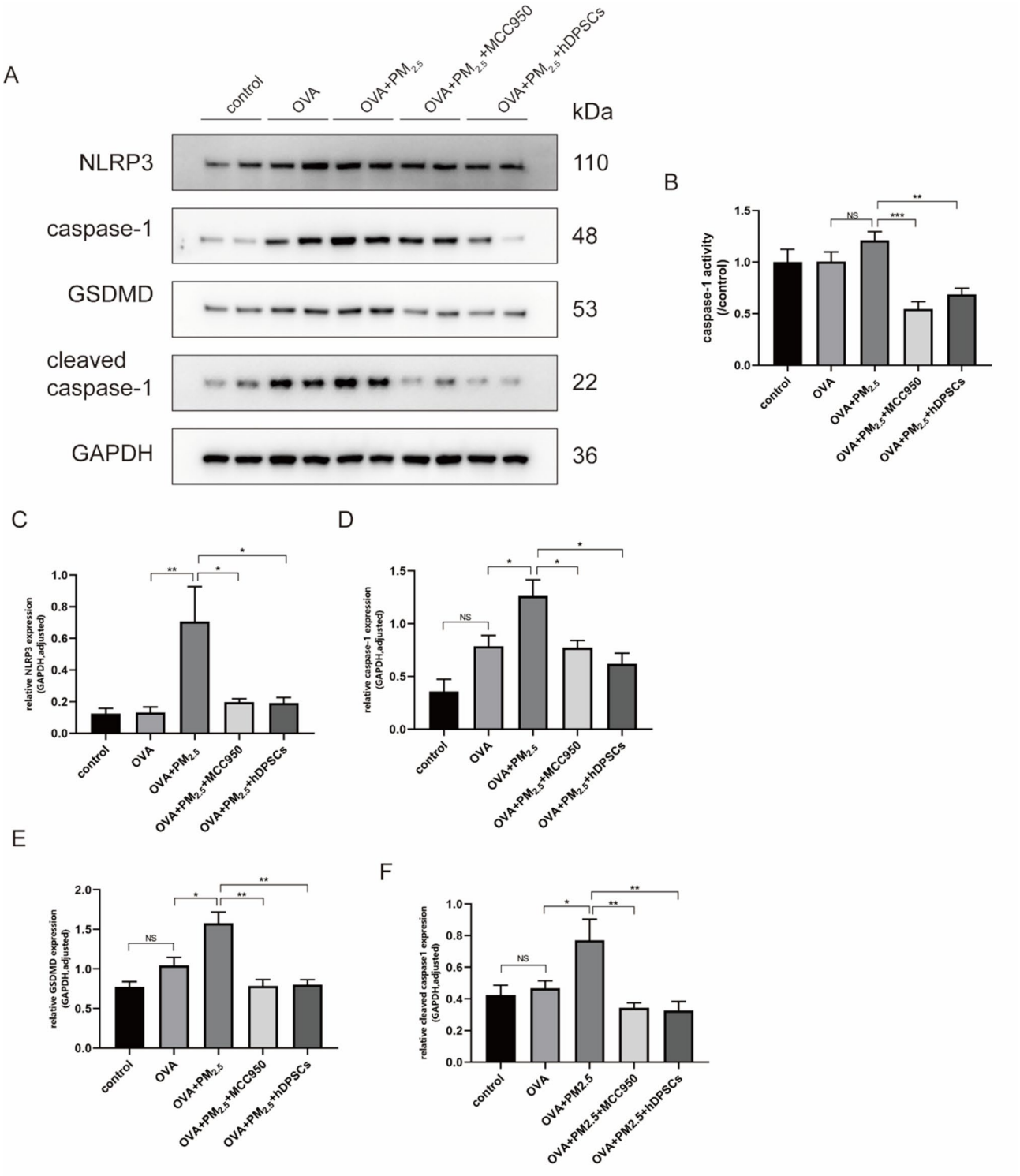

Fig. 7 HDPSCs infusion inhibited the expression of NLRP3 and downstream cytokines. (**A**) The protein concentrations of NLRP3, caspase-1, GSDMD, and cleaved caspase-1 in the lungs were detected using western blotting. (**B**) Caspase-1 activity in the lungs. (**C-F**) Relative expression of NLRP3, caspase-1, GSDMD, and cleaved caspase-1 standardized to GAPDH. ($n = 3$–5/group)

adjuvant mainly induces mice to generate a Th2-high response [42]. It is commonly known that the Th2 response and Th2 cytokines, including IL-4, IL-5, and IL-13, contribute to the development, maintenance and exacerbation of allergic asthma [44]. The primary function of IL-5 is to promote eosinophil proliferation, activation, and maturation [45]. IL-4 and IL-13 promote the production of allergen-specific IgE by B cells during allergic reactions [46]. Once allergen-specific IgE is released into the bloodstream and connects with allergic effector cells, a rapid hypersensitivity reaction occurs. Furthermore, the release of IL-4 and IL-13 can activate basophils and mast cells, resulting in pulmonary mucus hypersecretion and airway remodeling, which improves AHR and affects lung function. IL-13 secretion can lead to impaired epithelial barrier function, causing increased mucus production [47]. $PM_{2.5}$ is a prominent component of air pollution and can contribute to the development of several diseases [48]. $PM_{2.5}$ exposure has been demonstrated to worsened asthma [40, 49, 50]. Consistent with previous studies, the present study found that $PM_{2.5}$ intervention increased the levels of IL-4, IL-5 and IL-13, as well as serum IgE in the BALF of experimental asthmatic mice, increased mucus secretion, and increased the number of eosinophils in the BALF, confirming that $PM_{2.5}$ promotes the progression of experimental asthma.

Pyroptosis is a form of inflammatory cell death accompanied by cell swelling, membrane rupture and release of immunostimulatory molecules [10]. As a critical mediator of inflammatory responses, pyroptosis is predominantly executed through NLRP3 inflammasome activation, which exhibits significantly upregulated expression in $PM_{2.5}$-induced asthma exacerbation [43]. Upon activation, the NLRP3 inflammasome facilitates the maturation and extracellular secretion of pro-inflammatory cytokines IL-1β and IL-18 [51]. NLRP3-caspase-1-GSDMD is the typical pathway of pyroptosis, which is associated with a variety of inflammatory conditions [12]. NLRP3 inflammasome is triggered by $PM_{2.5}$ exposure. This cascade involves NLRP3-mediated caspase-1 activation, which subsequently cleaves GSDMD into N-terminal (GSDMD-N) and C-terminal (GSDMD-C), which then activated the downstream protein caspase-1 fragments. The GSDMD-N domain binds to membrane lipids, destroying their integrity and rupturing the cytosolic membrane, releasing inflammatory factors IL-1β and IL-18, resulting in pyroptosis [52]. This process not only eliminates intracellular pathogen niches but also propagates inflammation through release of cellular contents. In contrast, the expression of pyroptosis-related factors NLRP3, caspase-1, GSDMD, and cleaved caspase-1 were reduced after hDPSCs infusion, suggesting that hDPSCs may exert its anti-inflammatory effects by inhibiting NLRP3 inflammatory vesicle activation and pyroptosis. To further validate the role of NLRP3 inflammatory vesicles and pyroptosis in $PM_{2.5}$-induced asthma-exacerbated lung injury, we used the NLRP3 inflammatory inhibitor, MCC950 [53]. MCC950 was demonstrated to inhibit the ATP hydrolysis capacity of NLRP3, thereby preventing NLRP3-induced ASC oligomerization, which leads to caspase-1 activation and subsequent reduction in IL-1β release [35]. Previous results demonstrated that treatment with MCC950 in a mouse model of acute lung injury significantly reduced the maturation of NLRP3, caspase-1 and GSDMD and corresponding IL-1β release [54]. Consistent with previous findings, administration of the NLRP3 inhibitor MCC950 on top of OVA + $PM_{2.5}$ attenuated lung injury, mucus secretion as well as reduced expression of pyroptosis-related proteins.

Recent years have witnessed growing interest in mesenchymal stem cells (MSCs) as regenerative therapeutics for respiratory diseases [55]. Following intravenous administration, a proportion of mesenchymal stem cells exhibit pulmonary tropism, where they exert multifaceted therapeutic effects including restoration the lung microenvironment, protection alveolar epithelial cells and attenuation of fibrotic progression, demonstrating efficacy against COVID-19-associated pneumonia and pulmonary dysfunction [56]. Administration of MSCs in asthma model mice protects mice from chronic allergic airway inflammation, particularly by improving airway remodeling and preventing fibrosis [57]. In addition, it has been confirmed that MSCs exert their immunomodulatory role by modulating the TGF-β1/Smad signaling pathway in chronic allergic airway inflammation [58]. These cumulative findings robustly demonstrate the dual immunomodulatory and anti-inflammatory capacities of MSCs in respiratory pathophysiology.

Dental pulp stem cells, a type of mesenchymal stem cells, are the first human dental stem cells isolated from permanent teeth and have been shown to have therapeutic effects for many diseases [59–61]. Human dental pulp stem cells have been found to have anti-inflammatory properties [62]. Dental pulp stem cells were reported to attenuate CCL-induced cirrhosis by inhibiting GSDMD-mediated pyroptosis and inflammation [63]. In a previous study by our group, we found that the infusion of stem cells from human exfoliated deciduous teeth promoted the healing of tracheal fistula in rats and that intravenous infusion of pulp stem cells attenuated lung inflammation in rats with tracheal fistula [64]. Adult-derived dental pulp stem cells have a similar periodicity to that of stem cells from human exfoliated deciduous teeth [28]. Furthermore, it was found that dental pulp stem cells have beneficial effects in LPS-induced acute lung injury mouse model [65]. Our findings demonstrate that hDPSC administration effectively ameliorates $PM_{2.5}$-aggravated asthma by simultaneously reducing lung inflammation,

improving airway responsiveness, and suppressing Th2 cytokine production (IL-4, IL-5, and IL-13). Notably, hDPSCs exhibited comparable therapeutic efficacy to NLRP3 inhibitors by substantially reducing pulmonary expression of NLRP3, caspase-1, GSDMD, and cleaved caspase-1 along with subsequent decreases in IL-1β and IL-18 release. These findings strongly suggest that the anti-inflammatory effects of hDPSCs are mediated through inhibition of NLRP3 inflammasome-mediated pyroptosis.

There are some limitations to this study. The first limitation is that we did not establish a group with single hDPSCs treatment. Second, we did not perform in vitro cell culture experiments to confirm the effect of $PM_{2.5}$ and hDPSCs on cells. In addition, while our data demonstrate hDPSC-mediated pyroptosis suppression, the precise cellular communication mechanisms require further investigation.

Conclusion

In conclusion, our study demonstrates that hDPSCs could attenuate airway inflammation, mucus secretion, and protein leakage, in a $PM_{2.5}$-induced asthma exacerbation by suppressing the NLRP3-caspase-1-GSDMD signaling pathways, suggesting that hDPSCs could be a potential therapeutic strategy for $PM_{2.5}$ inhalation-mediated asthma.

Abbreviations

hDPSCs	Human dental pulp stem cells
PM2.5	Fine particulate matter
BALF	Bronchoalveolar lavage fluid
IL-1β	Interleukin-1β
IL-4	Interleukin-4
IL-6	Interleukin-6
NLRP3	The nod-like receptor pyrin domain containing 3

Supplementary Information

The online version contains supplementary material available at https://doi.org/10.1186/s13287-025-04368-5.

Supplementary Material 1

Supplementary Material 2

Acknowledgements

We thank all the investigators for their excellent assistance in this research. We thank Professor Kefang Lai and Dr. Chuqin Huang, from Guangzhou Institute of Respiratory Health for providing technical support for mouse lung function detection. The authors declare that they have not use AI-generated work in this manuscript.

Author contributions

J L, Y C conceived and designed the experiments. J L, Y C, Z L, Z L, A W, Z L and X L performed the experiments. J L analyzed the data and wrote the article. J W, F L and F W revised the manuscript. J W contributed to discussions and important reagents and supported funds. All authors read and approved the final manuscript.

Funding

The studies were supported by fundings from Jian Wu (National Natural Science Foundation of China (No.81970012), Natural Science Foundation of Guangdong Province (No. 2023A1515011587), and Project of Guangdong Provincial Department of Finance (No. KS0120220270).

Data availability

The datasets used and analyzed during the current study are available from the corresponding author upon reasonable request.

Declarations

Ethics approval and consent to participate

This study entitled "study on the effect and mechanism of human dental pulp stem cells on PM2.5-induced asthma exacerbations" was approved by the Animal Welfare and Use Committee of the South China University of Technology (Approval ID: 2023051) on July 26, 2023. Human dental pulp stem cells (HUXDP-01001, OriCell®) were present from Cyagen Biosciences (Guangzhou) Inc (https://www.oricellbio.cn/product/dental-pulp-msc-HUXDP-01001.html). At the same time, the donors had signed the informed consent forms.

Consent for publication

Not applicable.

Competing interests

The authors declare that they have no competing interests.

Author details

[1]Second Department of Elderly Respiratory, Guangdong Provincial People's Hospital, Southern Medical University, Guangzhou 510080, China
[2]School of Medicine, South China University of Technology, Guangzhou, Guangdong, China
[3]Critical Care Medicine Department, Sun Yat-Sen Memorial Hospital, Sun Yat-Sen University, Guangzhou 510120, China
[4]Joint Center for Regenerative Medicine Research of South China University of Technology and the University of Western Australia, School of Medicine, South China University of Technology, Guangzhou 515000, P.R. China
[5]The Sixth Affiliated Hospital, School of Medicine, South China University of Technology, Guangzhou 510000, P.R. China

Received: 5 November 2024 / Accepted: 25 April 2025
Published online: 13 May 2025

References

1. Stern J, Pier J, Litonjua AA. Asthma epidemiology and risk factors. Semin Immunopathol. 2020;42(1):5–15.
2. Reddel HK, Bacharier LB, Bateman ED, Brightling CE, Brusselle GG, Buhl R, et al. Global initiative for asthma strategy 2021: executive summary and rationale for key changes. Am J Respir Crit Care Med. 2022;205(1):17–35.
3. Porsbjerg C, Melén E, Lehtimäki L, Shaw D, Asthma. Lancet (London England). 2023;401(10379):858–73.
4. Guarnieri M, Balmes JR. Outdoor air pollution and asthma. Lancet (London England). 2014;383(9928):1581–92.
5. Rajagopalan S, Brook RD, Salerno PRVO, Bourges-Sevenier B, Landrigan P, Nieuwenhuijsen MJ, et al. Air pollution exposure and cardiometabolic risk. Lancet Diabetes Endocrinol. 2024;12(3):196–208.
6. Zanobetti A, Ryan PH, Coull BA, Luttmann-Gibson H, Datta S, Blossom J, et al. Early-Life exposure to air pollution and childhood asthma cumulative incidence in the ECHO CREW consortium. JAMA Netw Open. 2024;7(2):e240535.
7. Yang L, Li C, Tang X. The impact of PM2.5 on the host defense of respiratory system. Front Cell Dev Biology. 2020;8:91.
8. Huang D, Jia N, Pei C, Shen Z, Zhao S, Wang Y, et al. Rosavidin protects against PM2.5-induced lung toxicity via Inhibition of NLRP3 inflammasome-mediated pyroptosis by activating the PI3K/AKT pathway. Biochem Pharmacol. 2023;213:115623.
9. Huang D, Shi S, Wang Y, Wang X, Shen Z, Wang M, et al. Astragaloside IV alleviates PM2.5-caused lung toxicity by inhibiting inflammasome-mediated

pyroptosis via NLRP3/caspase-1 axis Inhibition in mice. Biomed Pharmacotherapy = Biomedecine Pharmacotherapie. 2022;150:112978.
10. Shao F. Gasdermins: making pores for pyroptosis. Nat Rev Immunol. 2021;21(10):620–1.
11. Swanson KV, Deng M, Ting JPY. The NLRP3 inflammasome: molecular activation and regulation to therapeutics. Nat Rev Immunol. 2019;19(8):477–89.
12. Liang X, Qin Y, Wu D, Wang Q, Wu H. Pyroptosis: a double-edged sword in lung cancer and other respiratory diseases. Cell Communication Signaling: CCS. 2024;22(1):40.
13. Xu K-Y, Wu C-Y, Tong S, Xiong P, Wang S-H. The selective Nlrp3 inflammasome inhibitor Mcc950 attenuates lung ischemia-reperfusion injury. Biochem Biophys Res Commun. 2018;503(4):3031–7.
14. Ren F, Xu J, Zhang J, Xu X, Huang L, Sun W, et al. PM2.5 induced lung injury through upregulating ROS-dependent NLRP3 Inflammasome-Mediated pyroptosis. Immunobiology. 2022;227(3):152207.
15. Li J, An Z, Song J, Du J, Zhang L, Jiang J, et al. Fine particulate matter-induced lung inflammation is mediated by pyroptosis in mice. Ecotoxicol Environ Saf. 2021;219:112351.
16. Xiong R, Jiang W, Li N, Liu B, He R, Wang B, et al. PM2.5-induced lung injury is attenuated in macrophage-specific NLRP3 deficient mice. Ecotoxicol Environ Saf. 2021;221:112433.
17. Lv F-J, Tuan RS, Cheung KMC, Leung VYL. Concise review: the surface markers and identity of human mesenchymal stem cells. Stem Cells. 2014;32(6):1408–19.
18. Mazziotta C, Badiale G, Cervellera CF, Tognon M, Martini F, Rotondo JC. Regulatory mechanisms of circular RNAs during human mesenchymal stem cell osteogenic differentiation. Theranostics. 2024;14(1):143–58.
19. Chu D-T, Phuong TNT, Tien NLB, Tran DK, Thanh VV, Quang TL, et al. An update on the progress of isolation, culture, storage, and clinical application of human bone marrow mesenchymal stem/stromal cells. Int J Mol Sci. 2020;21(3):708.
20. Chen W, He Z, Li S, Wu Z, Tan J, Yang W, et al. The effect of mesenchymal stem cells, adipose tissue derived stem cells, and cellular stromal vascular fraction on the repair of acute anal sphincter injury in rats. Bioeng (Basel Switzerland). 2022;9(7):318.
21. Araújo AB, Furlan JM, Salton GD, Schmalfuss T, Röhsig LM, Silla LMR, et al. Isolation of human mesenchymal stem cells from Amnion, chorion, placental decidua and umbilical cord: comparison of four enzymatic protocols. Biotechnol Lett. 2018;40(6):989–98.
22. Lv F, Lu M, Cheung KMC, Leung VYL, Zhou G. Intrinsic properties of mesemchymal stem cells from human bone marrow, umbilical cord and umbilical cord blood comparing the different sources of MSC. Curr Stem Cell Res Ther. 2012;7(6):389–99.
23. Zaripova LN, Midgley A, Christmas SE, Beresford MW, Pain C, Baildam EM, et al. Mesenchymal stem cells in the pathogenesis and therapy of autoimmune and autoinflammatory diseases. Int J Mol Sci. 2023;24(22):16040.
24. Leung VYL, Aladin DMK, Lv F, Tam V, Sun Y, Lau RYC, et al. Mesenchymal stem cells reduce intervertebral disc fibrosis and facilitate repair. Stem Cells. 2014;32(8):2164–77.
25. Brown C, McKee C, Bakshi S, Walker K, Hakman E, Halassy S, et al. Mesenchymal stem cells: cell therapy and regeneration potential. J Tissue Eng Regen Med. 2019;13(9):1738–55.
26. Gronthos S, Mankani M, Brahim J, Robey PG, Shi S. Postnatal human dental pulp stem cells (DPSCs) in vitro and in vivo. Proc Natl Acad Sci U S A. 2000;97(25):13625–30.
27. Poblano-Pérez LI, Castro-Manrreza ME, González-Alva P, Fajardo-Orduña GR, Montesinos JJ. Mesenchymal stromal cells derived from dental tissues: Immunomodulatory properties and clinical potential. Int J Mol Sci. 2024;25(4):1986.
28. Potdar PD, Jethmalani YD. Human dental pulp stem cells: applications in future regenerative medicine. World J Stem Cells. 2015;7(5):839–51.
29. Sun C, Cao C, Zhao T, Guo H, Fleming BC, Owens B, et al. A2M inhibits inflammatory mediators of chondrocytes by blocking IL-1β/NF-κB pathway. J Orthop Research: Official Publication Orthop Res Soc. 2023;41(1):241–8.
30. Geng P, Zhang Y, Zhang H, Dong X, Yang Y, Zhu X, et al. HGF-Modified dental pulp stem cells mitigate the inflammatory and fibrotic responses in Paraquat-Induced acute respiratory distress syndrome. Stem Cells Int. 2021;2021:6662831.
31. Gao X, Liu Z, Wang Z. Dental pulp stem cells ameliorate Elastase-Induced pulmonary emphysema by regulating inflammation and oxidative stress. J Inflamm Res. 2023;16:1497–508.
32. Schantz MM, Cleveland D, Heckert NA, Kucklick JR, Leigh SD, Long SE, et al. Development of two fine particulate matter standard reference materials (< 4 Mm and < 10 Mm) for the determination of organic and inorganic constituents. Anal Bioanal Chem. 2016;408(16):4257–66.
33. Wang A, Liu J, Li Z, Qian Z, Yang S, Luo S, et al. CC16 alleviates PM2.5-induced lung epithelial cell injury and airway inflammation in asthmatic mice by inhibiting ferroptosis. Ecotoxicol Environ Saf. 2025;289:117417.
34. Liu X, Li Z, Shan J, Wang F, Li Z, Luo S, et al. PM2.5 exposure inhibits transepithelial anion Short-circuit current by downregulating P2Y2 Receptor/CFTR pathway. Int J Med Sci. 2024;21(10):1929–44.
35. Coll RC, Hill JR, Day CJ, Zamoshnikova A, Boucher D, Massey NL, et al. MCC950 directly targets the NLRP3 ATP-hydrolysis motif for inflammasome Inhibition. Nat Chem Biol. 2019;15(6):556–9.
36. Firinci F, Karaman M, Baran Y, Bagriyanik A, Ayyildiz ZA, Kiray M, et al. Mesenchymal stem cells ameliorate the histopathological changes in a murine model of chronic asthma. Int Immunopharmacol. 2011;11(8):1120–6.
37. Xie T, Luo G, Zhang Y, Wang X, Wang X, Wu M, et al. Rho-kinase inhibitor fasudil reduces allergic airway inflammation and mucus hypersecretion by regulating STAT6 and NFκB. Clin Experimental Allergy: J Br Soc Allergy Clin Immunol. 2015;45(12):1812–22.
38. Cho K-S, Park M-K, Kang S-A, Park H-Y, Hong S-L, Park H-K, et al. Adipose-derived stem cells ameliorate allergic airway inflammation by inducing regulatory T cells in a mouse model of asthma. Mediators Inflamm. 2014;2014:436476.
39. Kurokawa A, Kondo M, Arimura K, Ashino S, Tagaya E. Less airway inflammation and goblet cell metaplasia in an IL-33-induced asthma model of leptin-deficient obese mice. Respir Res. 2021;22(1):166.
40. Zhao C, Wang Y, Su Z, Pu W, Niu M, Song S, et al. Respiratory exposure to PM2.5 soluble extract disrupts mucosal barrier function and promotes the development of experimental asthma. Sci Total Environ. 2020;730:139145.
41. Akar-Ghibril N, Casale T, Custovic A, Phipatanakul W. Allergic endotypes and phenotypes of asthma. J Allergy Clin Immunol Pract. 2020;8(2):429–40.
42. Lourenço LO, Ribeiro AM, Lopes FDTQDS, Tibério IFLC, Tavares-de-Lima W, Prado CM. Different phenotypes in asthma: clinical findings and experimental animal models. Clin Rev Allergy Immunol. 2022;62(1):240–63.
43. Zhang Y, Yang W, Li W, Zhao Y. NLRP3 inflammasome: checkpoint connecting innate and adaptive immunity in autoimmune diseases. Front Immunol. 2021;12:732933.
44. Komlósi ZI, van de Veen W, Kovács N, Szűcs G, Sokolowska M, O'Mahony L, et al. Cellular and molecular mechanisms of allergic asthma. Mol Aspects Med. 2022;85:100995.
45. Goetzl EJ. Th2 cells in rapid immune responses and protective avoidance reactions. FASEB Journal: Official Publication Federation Am Soc Experimental Biology. 2024;38(4):e23485.
46. Boonpiyathad T, Sözener ZC, Satitsuksanoa P, Akdis CA. Immunologic mechanisms in asthma. Semin Immunol. 2019;46:101333.
47. Heijink IH, Kuchibhotla VNS, Roffel MP, Maes T, Knight DA, Sayers I, et al. Epithelial cell dysfunction, a major driver of asthma development. Allergy. 2020;75(8):1902–17.
48. Arias-Pérez RD, Taborda NA, Gómez DM, Narvaez JF, Porras J, Hernandez JC. Inflammatory effects of particulate matter air pollution. Environ Sci Pollut Res Int. 2020;27(34):42390–404.
49. Celebi Sozener Z, Ozdel Ozturk B, Cerci P, Turk M, Gorgulu Akin B, Akdis M, et al. Epithelial barrier hypothesis: effect of the external exposome on the Microbiome and epithelial barriers in allergic disease. Allergy. 2022;77(5):1418–49.
50. Yang Y, Li X, An X, Zhang L, Li X, Wang L, et al. Continuous exposure of PM2.5 exacerbates ovalbumin-induced asthma in mouse lung via a JAK-STAT6 signaling pathway. Advances in clinical and experimental medicine. Official Organ Wroclaw Med Univ. 2020;29(7):825–32.
51. Chen Y, Ye X, Escames G, Lei W, Zhang X, Li M, et al. The NLRP3 inflammasome: contributions to inflammation-related diseases. Cell Mol Biol Lett. 2023;28(1):51.
52. Liu X, Xia S, Zhang Z, Wu H, Lieberman J. Channelling inflammation: gasdermins in physiology and disease. Nat Rev Drug Discovery. 2021;20(5):384–405.
53. Zahid A, Li B, Kombe AJK, Jin T, Tao J. Pharmacological inhibitors of the NLRP3 inflammasome. Front Immunol. 2019;10:2538.
54. Puri G, Naura AS. Implication of mitochondrial ROS-NLRP3 inflammasome axis during two-hit mediated acute lung injury in mice. Free Radic Res. 2022;56(1):1–16.
55. Zhou T, Yuan Z, Weng J, Pei D, Du X, He C, et al. Challenges and advances in clinical applications of mesenchymal stromal cells. J Hematol Oncol. 2021;14(1):24.

56. Leng Z, Zhu R, Hou W, Feng Y, Yang Y, Han Q, et al. Transplantation of ACE2- mesenchymal stem cells improves the outcome of patients with COVID-19 pneumonia. Aging Dis. 2020;11(2):216–28.
57. Takeda K, Webb TL, Ning F, Shiraishi Y, Regan DP, Chow L et al. Mesenchymal Stem Cells Recruit CCR2 + Monocytes To Suppress Allergic Airway Inflammation. Journal of Immunology (Baltimore, Md: 1950). 2018;200(4):1261-9.
58. Zhong H, Fan X-L, Fang S-B, Lin Y-D, Wen W, Fu Q-L. Human pluripotent stem cell-derived mesenchymal stem cells prevent chronic allergic airway inflammation via TGF-β1-Smad2/Smad3 signaling pathway in mice. Mol Immunol. 2019;109:51–7.
59. Zhu H, Xiong Y, Xia Y, Zhang R, Tian D, Wang T, et al. Therapeutic effects of human umbilical Cord-Derived mesenchymal stem cells in acute lung injury mice. Sci Rep. 2017;7:39889.
60. He Y, Li R, She W, Ai Y, Li K, Kumeria T, et al. Inhibitory effects of the nanoscale lysate derived from xenogenic dental pulp stem cells in lung cancer models. J Nanobiotechnol. 2023;21(1):488.
61. Dong X, Hu F, Yi J, Zhang Y, Liu C, Geng P, et al. DPSCs protect architectural integrity and alleviate intervertebral disc degeneration by regulating nucleus pulposus immune status. Stem Cells Int. 2022;2022:7590337.
62. Anderson S, Prateeksha P, Das H. Dental Pulp-Derived stem cells reduce inflammation, accelerate wound healing and mediate M2 polarization of myeloid cells. Biomedicines. 2022;10(8):1999.
63. Chen P, Zhou YK, Han CS, Chen LJ, Wang YM, Zhuang ZM, et al. Stem cells from human exfoliated deciduous teeth alleviate liver cirrhosis via Inhibition of gasdermin D-Executed hepatocyte pyroptosis. Front Immunol. 2022;13:860225.
64. Wang F, Li Z, Lyu F-J, Gao J, Lin J, Liu J, et al. The therapeutic effect of stem cells from human exfoliated deciduous teeth on a rat model of tracheal fistula. Stem Cell Res Ther. 2022;13(1):310.
65. Wakayama H, Hashimoto N, Matsushita Y, Matsubara K, Yamamoto N, Hasegawa Y, et al. Factors secreted from dental pulp stem cells show multifaceted benefits for treating acute lung injury in mice. Cytotherapy. 2015;17(8):1119–29.

Publisher's note